Closed orbits in axial symmetric Finslerian extension of a Schwarzschild black hole

Jin-Tao Yao[*] and Xin Li[†]

Department of Physics and Chongqing Key Laboratory for Strongly Coupled Physics, Chongqing University, Chongqing 401331, China

(Received 24 July 2023; accepted 5 October 2023; published 30 October 2023)

The axial symmetric Finslerian extension of a Schwarzschild spacetime is a generalization of Schwarzschild spacetime. It will return to Schwarzschild spacetime while the Finslerian parameter $\epsilon = 0$. Closed orbits are an important geometrical subject in mathematics that will help us to understand the physical properties of black holes in a strong gravitational region. The closed orbits of the axial symmetric Finslerian extension of a Schwarzschild black hole have been investigated in this paper. We have found that one necessary condition for the orbits of a Finslerian black hole to be closed is that the Finslerian parameter ϵ be rational. The numerical results of closed orbits of a Finslerian black hole are shown. They confirm our conclusion of the existence conditions of closed orbits.

DOI: 10.1103/PhysRevD.108.084067

I. INTRODUCTION

The black hole, as a prediction of general relativity, has played an important role in investigating gravitational physics. Penrose gave a robust proof for the general existence of black holes in mathematics [1]. Several astronomical observations have shown the physical existence of black holes. Accretion disks [2] can be used to locate supermassive compact objects, such as black holes. Gravitational waves can be generated from the merging of binary astronomical objects. The LIGO Scientific and Virgo Collaborations have detected gravitational waves from binary systems [3], which include the merging of binary black holes. The shadow of the supermassive black hole of M87 has been observed by the Event Horizon Telescope Collaboration [4]. Recently, pictures of the black hole shadow of Sagittarius (Sgr) A* have been released [5]. The Gravity Collaboration has observed orbits of several stars around Sgr A* with high precision [6]. They have detected Schwarzschild precession in the orbit of the star S2 [7].

The black hole, as a strong gravitational region, is a useful object for investigating possible properties and potential observable behaviors of various modified theories of gravity [8]. A succinct listing of such research subjects is given as follows. Quasinormal modes that carry intrinsic properties of black holes have been used to study holographic behaviors of black holes [9,10]. Observations of gravitational waves have been used to search for possible deviation from general relativity [11,12]. In modified theories of gravity, black hole shadows have been investigated [13–15]. Observational data of Schwarzschild precession in the orbit of the star S2 have been used to test the validity of the axial symmetric Finslerian extension of a Schwarzschild black hole [16]. Throughout this paper, we call this sort of Finslerian black hole a Finslerian Schwarzschild black hole for short.

The astronomical observations listed in the first paragraph are related to trajectories of gravitational objects. Therefore, one category of special orbits—namely, the periodical orbits—has drawn the interest of physicists. For example, it plays an important role in the study of gravitational waves [17]. In weak gravitational regions, the conditions allowing for periodical orbits of a Schwarzschild black hole are quite simple, since the orbits of the Schwarzschild black hole are confined to a plane. They exist if and only if the ratio of 2π to the Schwarzschild precession is rational. However, it is not a trivial task to find the conditions for the existence of periodical orbits in nonspherical black holes, and the properties of periodical orbits near the black hole become complicated even for Schwarzschild black holes. Inspired by these facts, Levin *et al.* have defined a taxonomy of orbits and found that each periodical orbit is characterized by a rational number [18]. This taxonomy has been used to study the periodical orbits of Kerr black holes [19], charged black holes [20], Kehagias-Sfetsos black holes [21], and hairy black holes in Horndeski's theory [22]. Thus, the taxonomy of orbits defined by Levin *et al.* provides a useful approach to investigating the properties of black holes in modified theories of gravity.

The other aspect, periodical orbits—called closed orbits—have been studied by mathematicians since a long

[*]yaojintao@stu.cqu.edu.cn
[†]lixin1981@cqu.edu.cn

 © 2023 American Physical Society

time ago. Poincaré has proved that there exists at least one closed geodesic on S^2 [23]. Poincaré's research has been extended to every compact Riemannian manifold by Lyusternik and Fet [24]. Mathematicians further conjecture that there exist infinitely many distinct prime closed geodesics on every compact Riemannian manifold. A review of mathematical researches on closed geodesics is given in Ref. [25].

Finsler geometry [26] is a natural generalization of Riemannian geometry. The gravitational theory based on Finsler geometry is expected not only to involve the contents of general relativity, but also to possess different features. The degree of freedom of Finsler geometry is higher than that of Riemannian geometry. Therefore, different Finslerian gravitational field equations have been proposed [27–30]. These gravitational field equations need to be falsified or constrained by physical observations. One approach is studying the extension of Schwarzschild spacetime. Various Finslerian extensions of Schwarzschild spacetime have been proposed and discussed [31–33]. Based on the Finslerian gravitational field equation proposed by Rutz [28], we have found a Finslerian extension of the Schwarzschild black hole [34]. A Finslerian Reissner-Nordström black hole has also been found [35]. The above black hole solutions found by us violate spherical symmetry and preserve axial symmetry. Such features reflect on their quasinormal modes [36,37]. The orbits of Finslerian Schwarzschild black holes have been investigated [16]. Due to the symmetry of the Finslerian Schwarzschild black hole, its orbits exhibit both orbital precession and orbital plane precession. Furthermore, the Finslerian parameter which describes the deviation from Schwarzschild spacetime has been constrained by the observations of the Gravity Collaboration [7].

The orbits of Finslerian Schwarzschild black holes have been investigated in weak gravitational regions [16]. However, it is of interest to study them in strong gravitational regions. Also, the closed geodesics problem in Finsler geometry is quite different from the one in Riemannian geometry. Katok has found some irreversible Finsler metrics in which there exist finitely many distinct closed geodesics [38]. The existence of at least two closed geodesics on Finsler 2-spheres has been solved in Ref. [39]. Therefore, it is of interest in both physics and math to study whether or not closed geodesics exist in Finslerian Schwarzschild black holes.

This paper is organized as follows: In Sec. II, we introduce the basic concept of Finslerian Schwarzschild black holes and discuss their geodesic equations. In Sec. III, we first give a general discussion of closed orbits. Then, we investigate the orbits on the equatorial plane of a Finslerian Schwarzschild black hole. This gives us a somewhat direct physical picture by Levi's taxonomy [18]. At the end of the section, we investigate general 3D orbits of Finslerian Schwarzschild black holes and study the influences of the Finslerian parameter ϵ on 3D closed orbits. Finally, we summarize the research results in Sec. IV.

II. GEODESICS OF FINSLERIAN SCHWARZSCHILD SPACETIME

In Finsler geometry, the basic element is Finsler structure F. To guarantee that the length of Finsler geometry $\int F d\tau$ is independent of the choice of curve parameter τ, it satisfies $F(x, \lambda y) = \lambda F(x, y)$ for all $\lambda > 0$, where $x \in \mathcal{M}$ ($\mathcal{M}$ is the Finsler manifold) represents position and $y \equiv dx/d\tau$ represents velocity [26]. The Finslerian metric is given as

$$g_{\mu\nu} \equiv \frac{\partial}{\partial y^\mu}\frac{\partial}{\partial y^\nu}\left(\frac{1}{2}F^2\right). \tag{1}$$

In physics, the Finslerian length is not required to be positive definite. The Finsler metric with a Lorentz signature has been discussed in Ref. [40]. A positive, zero, or negative F corresponds to spacelike, null, or timelike curves, respectively. The geodesic equation originates from the variation of Finslerian length, which is a unique definition in Finsler geometry [26]. The geodesic equation that preserves the Finsler structure is given as

$$\frac{d^2x^\mu}{d\tau^2} + 2G^\mu = 0, \tag{2}$$

where

$$G^\mu = \frac{1}{4}g^{\mu\nu}\left(\frac{\partial^2 F^2}{\partial x^\lambda \partial y^\nu}y^\lambda - \frac{\partial F^2}{\partial x^\nu}\right) \tag{3}$$

is called the geodesic spray coefficient. In Finsler geometry, there is a geometrical invariant—namely, the Ricci scalar. It is insensitive to various connections that one can choose in Finsler geometry [26]. It is of the form

$$Ric \equiv R^\mu_\mu = \frac{1}{F^2}\left(2\frac{\partial G^\mu}{\partial x^\mu} - y^\lambda\frac{\partial^2 G^\mu}{\partial x^\lambda \partial y^\mu} + 2G^\lambda\frac{\partial^2 G^\mu}{\partial y^\lambda \partial y^\mu} - \frac{\partial G^\mu}{\partial y^\lambda}\frac{\partial G^\lambda}{\partial y^\mu}\right). \tag{4}$$

The Finslerian gravitational vacuum field equation proposed by Rutz [28] is the vanishing of the Ricci scalar—namely, $Ric = 0$. One exact solution of Rutz's field equation—namely, the Finslerian Schwarzschild solution—is given as [34]

$$F^2 = -f(r)y^t y^t + f(r)^{-1}y^r y^r + r^2\bar{F}^2, \tag{5}$$

where $f(r) = 1 - \frac{2GM}{r}$, M denotes the mass of the black hole, and $\bar{F}$ satisfies the following specific form:

$$\bar{F} = \frac{\sqrt{(1-\epsilon^2\sin^2\theta)y^\theta y^\theta + \sin^2\theta y^\varphi y^\varphi}}{1-\epsilon^2\sin^2\theta} - \frac{\epsilon\sin^2\theta y^\varphi}{1-\epsilon^2\sin^2\theta}. \tag{6}$$

$\bar{F}$ is a two-dimensional Finsler space with positive constant flag curvature. This Finsler space (6) was proposed in Refs. [38,41]. It has been shown that this Finsler space (6) has two geometrically distinct closed geodesics if the Finslerian parameter ϵ is irrational [42].

By plugging the Finslerian Schwarzschild metric (5) into the general form of geodesic equation (2) in Finsler spacetime, we can obtain the specific form of the geodesic equations of Finslerian Schwarzschild spacetime. It is given as follows:

$$\frac{d^2t}{d\tau^2}+\frac{f'}{f}\frac{dt}{d\tau}\frac{dr}{d\tau}=0, \tag{7}$$

$$\frac{d^2r}{d\tau^2}+\frac{ff'}{2}\left(\frac{dt}{d\tau}\right)^2-\frac{f'}{2f}\left(\frac{dr}{d\tau}\right)^2-rf\bar{F}^2=0, \tag{8}$$

$$\frac{d^2\theta}{d\tau^2}+\frac{2}{r}\frac{dr}{d\tau}\frac{d\theta}{d\tau}-\frac{\sin\theta\cos\theta}{1-\epsilon^2\sin^2\theta}\left(\epsilon^2\left(\frac{d\theta}{d\tau}\right)^2+\left(\frac{d\varphi}{d\tau}\right)^2 -2\epsilon\bar{F}\frac{d\varphi}{d\tau}\right)=0, \tag{9}$$

$$\frac{d^2\varphi}{d\tau^2}+\frac{2}{r}\frac{dr}{d\tau}\frac{d\varphi}{d\tau}+2\cot\theta\frac{d\theta}{d\tau}\left(\frac{d\varphi}{d\tau}-\epsilon\bar{F}\right)=0, \tag{10}$$

where the prime denotes differentiation with respect to the coordinate r. Due to the symmetry of Finslerian Schwarzschild spacetime [34], we obtain four constants of motion from the geodesic equations. The geodesic equations for massive particles are given as [16]

$$\dot{t}=E/\left(1-\frac{2GM}{r}\right), \tag{11}$$

$$\dot{r}^2=E^2-\left(1-\frac{2GM}{r}\right)\left(1+\frac{K^2}{r^2}\right), \tag{12}$$

$$\dot{\theta}^2=\frac{K^2}{r^4}\left(\frac{\sin^2\theta(K-\epsilon J)^2-J^2}{\sin^2\theta(K-\epsilon J)^2}\right), \tag{13}$$

$$\dot{\varphi}=\frac{K}{r^2}\left(\frac{\epsilon\sin^2\theta(K-\epsilon J)+J}{\sin^2\theta(K-\epsilon J)}\right), \tag{14}$$

where the overdot denotes differentiation with respect to the proper time τ. The constants E and J originate from Killing vectors of Finslerian Schwarzschild black holes [34] and denote the energy and angular momentum of particles, respectively. The constant K stems from the geometric structure of Finslerian Schwarzschild spacetime [16]. The fourth constant represents the normalization constant for geodesics. The orbital motion of massive particles is investigated in this paper, hence the choice of $F^2=-1$.

The Finslerian parameter ϵ describes the deviation between a Finslerian Schwarzschild black hole and a Schwarzschild black hole. In general, the Finslerian parameter ϵ will affect both orbital precession and orbital plane precession. It implies that the orbits of a Finslerian Schwarzschild black hole are not confined to a single plane. Therefore, an inclination angle exists in Finslerian Schwarzschild spacetime. The inclination angle ι ($\iota\equiv\frac{\pi}{2}-\theta_{\min}$) can be derived from Eq. (13) by requiring that $\dot{\theta}=0$. It is given as

$$\cos\iota=1/(n-\epsilon), \tag{15}$$

where $n\equiv|K/J|$.

III. CLOSED ORBITS OF FINSLERIAN SCHWARZSCHILD BLACK HOLES

The general definition of closed orbits is given by Poincaré [43]: For an orbit $f(x,\dot{x};t)$, if there exists a minimum and finite time $T>0$, such that $f(x,\dot{x};t)=f(x,\dot{x};t+T)$, where x and $\dot{x}$ represent the generalized coordinate and generalized velocity of the orbit, respectively, such an orbit is a *closed orbit* [43], and T is the period of this orbit.

According to the research of Ref. [18], closed orbits are related to rational numbers. This relation can be clearly specified by the example of a clock. The rotation of a hand on a clock can be described by one of two classes. The hand will return to its start point in a finite step if the ratio of each rotated arc length of the hand to the arc length of the circle is rational; we call this class *rational rotation*. The hand cannot return to its start point in a finite step if the ratio of each rotated arc length of the hand to the arc length of the circle is irrational; we call this class *irrational rotation*. Therefore, the closed geodesic of Schwarzschild spacetime in a weak field region exists if and only if its precession is a rational rotation—namely, the ratio of precession to 2π must be rational.

The existence conditions for a closed geodesic in three spatial dimensions are much more complicated. However, due to the four constants of motion in Finslerian Schwarzschild spacetime, the existence conditions for a closed geodesic can be clearly specified. In a bounded geodesic, we can find from the four constants of motion that there are three periods for the geodesic of Finslerian Schwarzschild spacetime. The first period is related to radial motion, which can be derived from Eq. (12) by requiring $\dot{r}=0$. It is the period from periastron r_p to apastron r_a. The second period is related to zenithal motion, which is the period from the minimum inclination angle (15) to its maximum. It describes the period of the inclination plane of the geodesics. The last period is obvious—it is the period of the azimuth of the particle. Similar to the discussion in two dimensions, the closed geodesic of Finslerian Schwarzschild spacetime in three spatial dimensions exists if and only if the ratios between two pairs of the three periods are rational.

A. Closed orbits on equatorial plane

Finslerian Schwarzschild spacetime (5) possesses similar properties to Kerr spacetime, such as symmetry [34], quasinormal modes [36,37], and orbital motions [16]. Thus, special orbital motions exist in Finslerian Schwarzschild spacetime—namely, they are confined to the equatorial plane if the initial position and velocity of the particle are located at the equatorial plane. One can find from Eq. (13) that only one of the two constants J and K is independent in the equatorial plane. And the two constants satisfy the following relations, which can be derived directly from Eq. (13):

$$K = J(\epsilon \pm 1). \tag{16}$$

This fact implies that the orbits on the equatorial plane have a lower degree of freedom than the general 3D orbits in Finslerian Schwarzschild spacetime. For simplicity, we first investigate a closed orbit on the equatorial plane. Following the research of Ref. [18], the periodicity of orbits on the equatorial plane ($\theta = \frac{\pi}{2}$) is characterized by the radial frequency ω_r and the azimuthal frequency ω_φ. We first introduce a new time variable which is similar to Mino time [19]—namely, $d\lambda \equiv d\tau/r^2$, such that each of $r(\lambda)$ and $\theta(\lambda)$ is independently periodic. The azimuthal frequency is defined as

$$\omega_r \equiv \frac{2\pi}{\Lambda_r}, \tag{17}$$

where

$$\Lambda_r = \oint_r d\lambda = 2\int_{r_p}^{r_a} \frac{dr}{\sqrt{E^2 r^4 - r^2 f(r)(r^2 + K^2)}} \tag{18}$$

is the radial period. Associated with the radial period, the definition of ω_φ over one radial period is

$$\omega_\varphi \equiv \frac{1}{\Lambda_r}\int_0^{\Lambda_r} d\varphi. \tag{19}$$

By making use of the geodesic equations (12) and (14), and noticing that $\theta = \frac{\pi}{2}$, the value of ω_φ (19) can be derived as the integration of r. It is given as

$$\omega_\varphi = \frac{\Delta\varphi}{\Lambda_r}, \tag{20}$$

where

$$\Delta\varphi = \oint_r d\varphi = 2(1+\epsilon)\int_{r_p}^{r_a} \frac{K}{\sqrt{E^2 r^4 - r^2 f(r)(r^2 + K^2)}} dr \tag{21}$$

is the accumulated azimuth over one radial period. The integral in formula (21) is a positive real multiple of 2π. It should be noticed that the ratios between frequencies used in our study are independent of the selection of time variable.

On the equatorial plane, only two frequencies, ω_φ and ω_r, remain. The above discussions imply that closed orbits exist if the ratio between these two frequencies is rational. Following the research of Ref. [18], the ratio is given as

$$q \equiv \frac{\omega_\varphi}{\omega_r} - 1 = \frac{\Delta\varphi}{2\pi} - 1. \tag{22}$$

One can find from the formula (21) that the Finslerian parameter ϵ plays an important role in determining whether the parameter q is rational or not. In general, a rational ϵ is one necessary condition for q being rational. If ϵ is irrational, then q is rational only if the integral in formula (21) is of the form $(1+\epsilon)^{-1} \times 2\pi A$, where A is a rational constant. Such conditions cannot be generally fulfilled.

In the following, we will use numerical results to show the existence of closed orbits of a Finslerian Schwarzschild black hole on the equatorial plane. For convenience, we use the geometrized units ($G = c = 1$) in numerical calculations and the conventional choice of $M = 1$. In this case, the Schwarzschild radius $r_s = 2$. Following the spirit of taxonomy in Ref. [18], the q of an equatorial periodic orbit in Finslerian Schwarzschild spacetime can be interpreted as three integers (z, w, v):

$$q = w + \frac{v}{z}. \tag{23}$$

This definition has been discussed in previous works [18,20,21,44–46] and has demonstrated its superiority. Each integer is a geometric feature. Namely, the integers z, w, and v represent the zoom number, the whirls number, and the vertex number at which a radial period ends, respectively. Note that the geometric features of q lie only on the equatorial plane—i.e., the $r\cos\varphi - r\sin\varphi$ plane.

So as to exhibit the geometric features represented by the three integers (z, w, v), A series of $w = 1$ visualization results of bound orbits with $K = 3.9$ around the Finslerian Schwarzschild black hole are shown in Fig. 1. The Finslerian parameters are $\epsilon = 0.5$ for row 1 and $\epsilon = 1/\sqrt{3.975}$ for row 2. The energy in each graph is $E = 0.976525$, 0.981012, 0.982507 from left to right, and graphs in the same column have the same energy. A distinct feature is that after finding (z, w, v) according to Eq. (23), the number of leaves in the orbit is directly indicated by the integer z. As the number of leaves

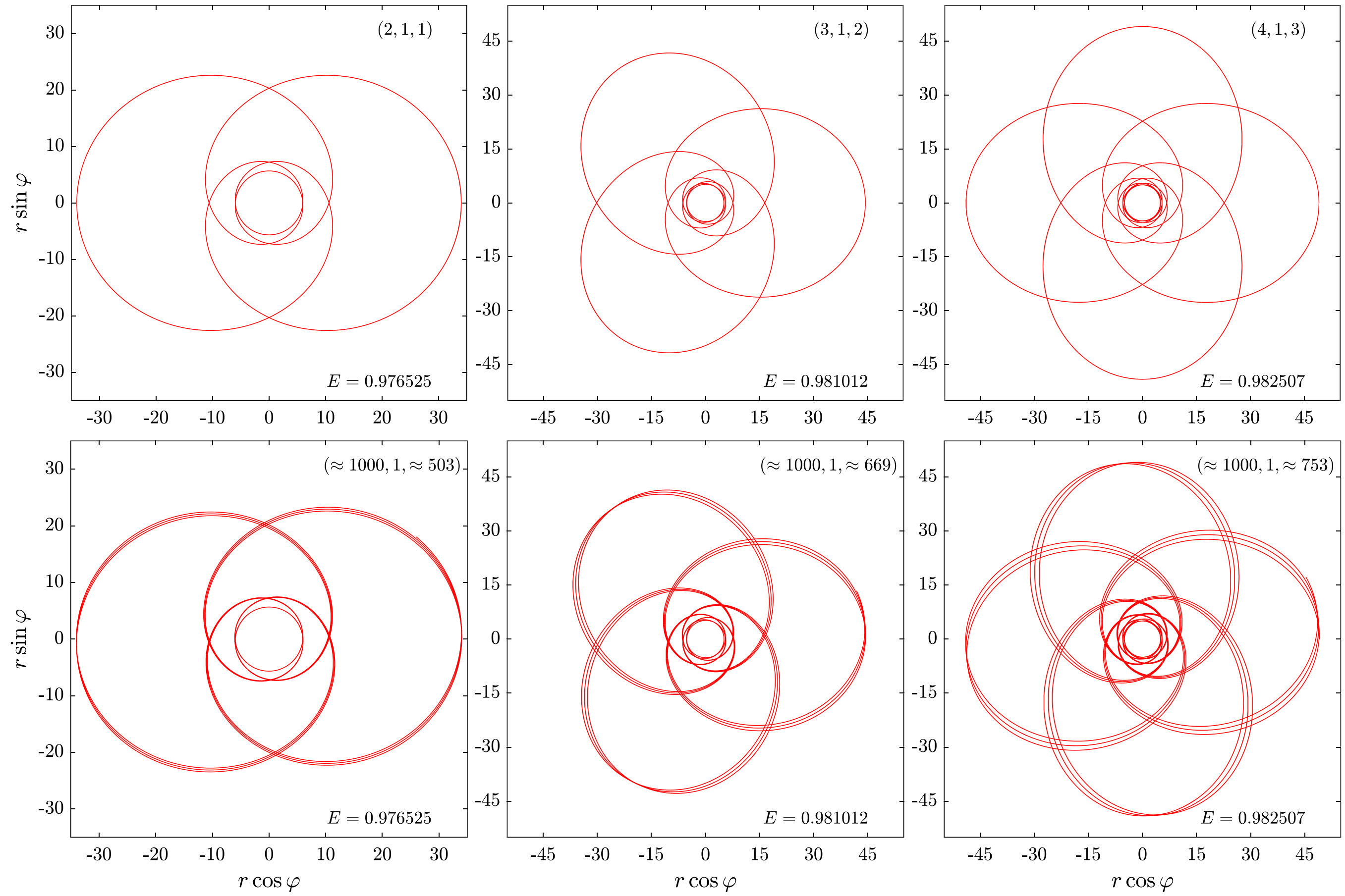

FIG. 1. A series of equatorial orbits with $K = 3.9$. The Finslerian parameters ϵ for rows 1 and 2 are 0.5 and $1/\sqrt{3.975}$, respectively. The energy in each graph is $E = 0.976525, 0.981012, 0.982507$ from left to right, and graphs in the same column have the same energy. The three numbers within brackets in each figure denote (z, w, v). The unit length of each plot is 0.5 Schwarzschild radii.

increases with value of z, the orbital structure becomes more complex. As shown in Fig. 1, when we change $\epsilon = 0.5$ to a irrational number $1/\sqrt{3.975}$ near 0.5 while keeping other parameters unchanged, the periodic orbits in row 1 become the aperiodic orbits in row 2, which can be regarded as the precession of the periodic orbit. Every computer program truncates numbers to a finite precision; this makes the calculation of an aperiodic orbit indistinguishable from some periodic orbits. So, when z becomes large after the parameters are fine-tuned, one can approximate it as an aperiodic orbit.

B. 3D closed orbits

The general 3D orbits are investigated in this subsection. Because the general 3D orbits exhibit intricate three-dimensional motion, three frequencies need to be considered. As discussed in the beginning of this section, the orbit will be closed when the three orbital frequencies are rationally related to each other.

The definition of radial frequency ω_r is the same as that in Sec. III A. The definition of zenithal frequency is given as

$$\omega_\theta \equiv \frac{2\pi}{\Lambda_\theta}, \tag{24}$$

where

$$\Lambda_\theta = \oint_\theta d\lambda = \frac{4}{K}\int_{\theta_{\min}}^{\pi/2} \frac{\sin\theta(K-\epsilon J)}{\sqrt{\sin^2\theta(K-\epsilon J)^2 - J^2}} d\theta = \frac{2\pi}{K} \tag{25}$$

is the zenithal period, which is similar to the Mino period defined in Ref. [19]. The ratio $q_{r\theta}$ between the zenithal and radial frequencies is given as

$$\begin{aligned} q_{r\theta} &\equiv \frac{\omega_\theta}{\omega_r} - 1 \\ &= \frac{K}{2\pi}\Lambda_r - 1, \end{aligned} \tag{26}$$

this parameter describes the geometric features of the track on the orbital plane. The definition of *orbital plane* has been given in detail in the Appendix. One necessary condition for closed orbits is that $q_{r\theta}$ be rational.

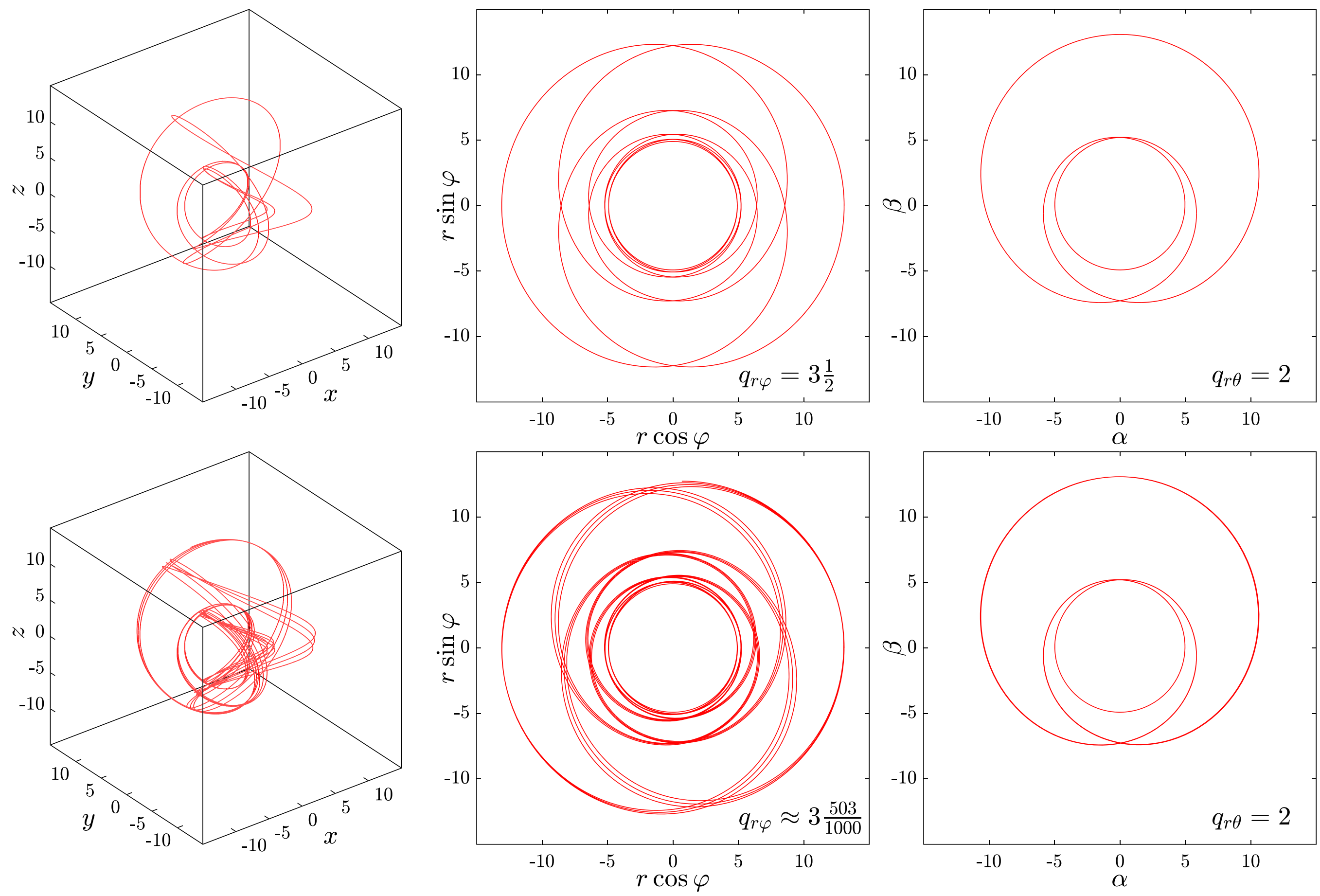

FIG. 2. A series of $E = 0.954609$, $K = 3.6$, $J = 1.2$, and $r_0 = 13.085189$ orbits. Column 1 shows the full 3D orbit. Column 2 displays the 3D orbit maps on the equatorial plane. Column 3 is the projection of the 3D orbit onto the orbital plane. The Finslerian parameters are $\epsilon = 0.5$ and $\epsilon = 1/\sqrt{3.95}$ for rows 1 and 2, respectively. The (α, β) axes in column 3 are the projection coordinates of the 3D orbit on the orbital plane. The unit length of each plot is 0.5 Schwarzschild radii.

The $q_{r\theta}$ of a closed orbit can also be decomposed into three integers (z, w, v), and each integer represents the same meaning as the previous one, but the geometric features they represent are on the orbital plane. To show these geometric features, we plot the projection of two 3D orbits on the orbital plane in the third column of Fig. 2; the (α, β) axes in the third column are the projection coordinates of the 3D orbit on the orbital plane (See the Appendix for details). Three-dimensional periodic and aperiodic orbits are distinguished in the same way as equatorial orbits—rows 1 and 2 of column 1 in Fig. 2 are the 3D periodic orbit and aperiodic orbit, respectively. As can be seen, the periodicity of a orbit on the orbital plane will not be affected when only the Finslerian parameter is changed, which is consistent with Eq. (26). In addition, Fig. 2 also shows that when some special orbital parameters are selected, the periodic orbit and the aperiodic orbit will correspond to the same rational $q_{r\theta}$. So, it is necessary to study the periodicity of φ motion while $q_{r\theta}$ is rational.

Azimuthal motion of a 3D orbit is different from radial motion and zenithal motion, which can be made independent by choosing an appropriate time variable. Both radial motion and zenithal motion will affect the periodicity of the azimuth. The rational $q_{r\theta}$ is necessary for searching the 3D closed orbits. Therefore, it is convenient to study the periodic behavior of φ in a time range $[\lambda, \lambda + \Lambda]$ where both $r(\lambda)$ and $\theta(\lambda)$ are closed. The selection of Λ satisfies the following conditions:

$$\Lambda = N\Lambda_r = M\Lambda_\theta, \tag{27}$$

where M and N are both positive integers and mutually prime, such that

$$r(\lambda + \Lambda) = r(\lambda), \qquad \theta(\lambda + \Lambda) = \theta(\lambda), \tag{28}$$

and then

$$\dot{t}(\lambda + \Lambda) = \dot{t}(\lambda), \qquad \dot{r}(\lambda + \Lambda) = \dot{r}(\lambda), \tag{29}$$

$$\dot{\theta}(\lambda + \Lambda) = \dot{\theta}(\lambda), \qquad \dot{\varphi}(\lambda + \Lambda) = \dot{\varphi}(\lambda), \tag{30}$$

where the overdot denotes differentiation with respect to the time variable ($d\lambda = d\tau/r^2$), which is similar to Mino time.

Each bound orbit has two radial turning points, r_p and r_a, and two zenithal turning points, $\theta_{\min}$ and $\theta_{\max}$; the orbit oscillates in the region bounded by these points. Inspired by Refs. [47–49], the accumulated azimuth during a Λ is

$$\Delta\Phi = N \oint_r \frac{\epsilon K}{\pm_{\dot{r}} \sqrt{E^2 r^4 - r^2 f(r)(r^2 + K^2)}} dr + M \oint_\theta \frac{J}{\pm_{\dot{\theta}} \sin\theta \sqrt{\sin^2\theta (K - \epsilon J)^2 - J^2}} d\theta, \tag{31}$$

where $\oint_r$ and $\oint_\theta$ represent integration in a radial and zenithal period, respectively. $\pm_{\dot{r}}$ and $\pm_{\dot{\theta}}$ indicate the signs of $\dot{r}$ and $\dot{\theta}$, which switch at radial and zenithal turning points, respectively. The second term on the right side of Eq. (31) is integrable, and the result of integration is

$$M \oint_\theta \frac{J}{\pm_{\dot{\theta}} \sin\theta \sqrt{\sin^2\theta (K - \epsilon J)^2 - J^2}} d\theta = 2M\pi. \tag{32}$$

Therefore, by plugging Eqs. (25) and (27) into Eq. (31), we obtain

$$\Delta\Phi = \epsilon K N \Lambda_r + 2M\pi = (1+\epsilon) K N \Lambda_r = (1+\epsilon) K M \Lambda_\theta. \tag{33}$$

Then, the azimuthal frequency Ω_φ over one common period Λ of radial motion and zenithal motion is

$$\Omega_\varphi = \frac{1}{\Lambda} \int_0^\Lambda d\varphi = \frac{\Delta\Phi}{\Lambda} = (1+\epsilon) K. \tag{34}$$

Because Λ is a positive integer multiple of Λ_r, the form of radial frequency for a 3D orbit is the same as with ω_r (17). Analogously to the equatorial orbit, one can introduce a ratio to describe the relationship between the radial motion and azimuthal motion. It is of the form

$$q_{r\varphi} = \frac{\Omega_\varphi}{\omega_r} - 1 = \frac{(1+\epsilon)K}{2\pi} \Lambda_r - 1. \tag{35}$$

When $q_{r\varphi}$ is a rational number, the accumulated azimuth during a Λ is a rational multiple of 2π, so the particle will return to its starting point after a finite number of Λ's, and the velocity is the same as the initial conditions. When $q_{r\varphi}$ is a irrational number, the space coordinates and velocity of the particle cannot be the same as the initial conditions at the same time, so the orbit is aperiodic. Due to the accumulated azimuth of a 3D orbit over one radial period not necessarily being a constant, as shown in Figs. 2 and 3, $q_{r\varphi}$ cannot be decomposed into three integers like q and $q_{r\theta}$ to describe the geometric characteristics of a 3D orbit.

Combining the formulas of $q_{r\theta}$ (26) and $q_{r\varphi}$ (35), we find that

$$q_{r\varphi} = (1+\epsilon) q_{r\theta} + \epsilon. \tag{36}$$

Therefore, $q_{r\varphi}$ is rational if both ϵ and $q_{r\theta}$ are rational. In summary, one necessary condition for the 3D orbits of a Finslerian Schwarzschild black hole to be closed is that the Finslerian parameter ϵ be rational.

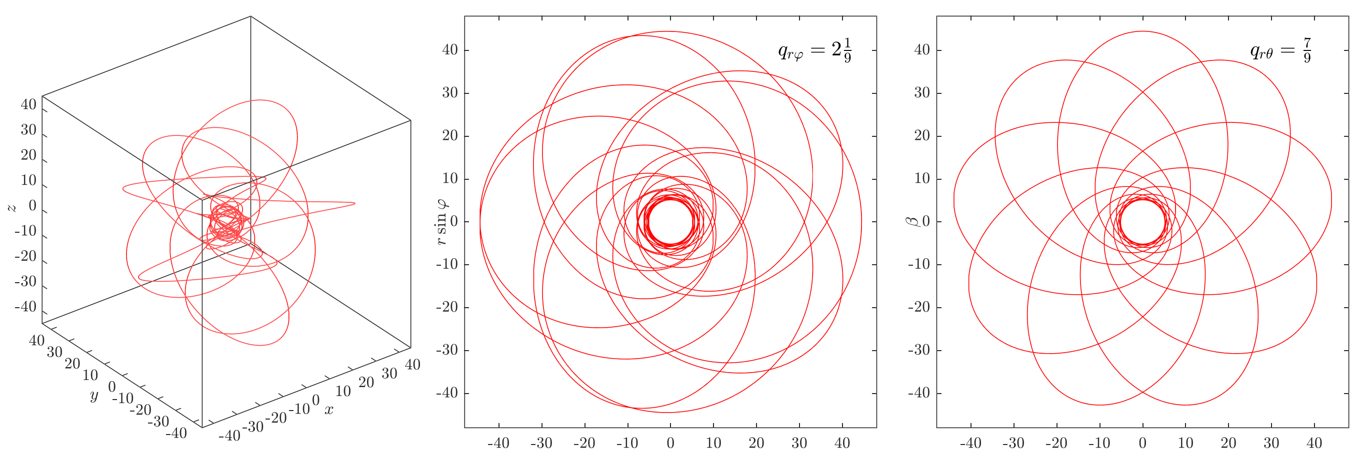

FIG. 3. 3D periodic orbit with $\epsilon = 0.75$, $K = 3.9$, $E = 0.981012$, and $J = 1.5$. The left graph displays the full 3D orbit, the center one is the projection onto the $r\cos\varphi - r\sin\varphi$ plane, and the right graph gives the projection onto the orbital plane. The initial conditions are: $r_0 = r_a = 44.488915$, $\theta_0 = \theta_{\min} = 0.571079$, and $\varphi_0 = 0$. The axes (α, β) in the right graph are the projection coordinates of the 3D orbit onto the orbital plane. The unit length of each plot is 0.5 Schwarzschild radii.

IV. CONCLUSIONS

In this paper, we have investigated the closed orbits of Finslerian Schwarzschild black holes (5). For the special symmetry of a Finslerian Schwarzschild black hole, four constants of motion—(11), (12), (13), and (14)—are derived from the geodesic equations. We have used a clock as an example to indicate how the closed orbits are related to the rational numbers. The closed geodesic in Finslerian Schwarzschild spacetime in three spatial dimensions exists if and only if the ratios between two pairs of the three periods are rational. In fact, only two ratios are independent. We have found that the two ratios satisfy the relation in Eq. (36). This implies that one necessary condition for the 3D orbits of a Finslerian Schwarzschild black hole to be closed is that the Finslerian parameter ϵ be rational.

Following the taxonomy of closed orbits in Ref. [18], we have obtained numerical results for closed orbits on the equatorial plane. They are shown in Fig. 1. The numerical results of 3D closed orbits are shown in Figs. 2 and 3. It should be noticed that every number calculated in a computer program has finite precision, which means these numbers are rational. Thus, the orbits shown in Figs. 1–3 all seem to be closed. However, these figures show that the periodicity of orbits change dramatically even for two close Finslerian parameters ϵ in which one is rational and another is irrational. This fact confirms our conclusion of the existence conditions for the closed orbits of Finslerian Schwarzschild black holes.

ACKNOWLEDGMENTS

This work has been supported by the National Natural Science Fund of China (Grants No. 12275034 and No. 12147102).

APPENDIX: DEFINITION OF THE ORBITAL PLANE

The orbital plane is involved in the study of periodic $r-\theta$ motion. The orbital plane is an instantaneous plane defined as a plane in the tangent space spanned by $\vec{R}$ and $\vec{P}$. This plane is perpendicular to the corresponding angular momentum $\vec{\mathcal{L}}=\vec{R}\times\vec{P}$ all the time.

We convert spherical coordinates to Cartesian coordinates:

$$\begin{aligned}\vec{R}&=(x,y,z)\\&=(r\sin\theta\cos\varphi, r\sin\theta\sin\varphi, r\cos\theta).\end{aligned}\tag{A1}$$

Then,

$$\vec{\mathcal{L}}=\vec{R}\times\vec{P},\tag{A2}$$

where

$$\vec{P}=(P_x,P_y,P_z),\tag{A3}$$

for which

$$P_i=\frac{\partial R_i}{\partial q^\nu}\eta^{\mu\nu}P_\mu,\tag{A4}$$

where $i=x, y, z$ and $\mu,\nu=r,\theta,\varphi$. As shown in Eq. (A1), we use the coordinate transformation from spherical coordinates to Cartesian coordinates, so the terms $\eta^{\mu\nu}$ in Eq. (A4) should be derived from the metric

$$(\eta_{\mu\nu})=\begin{pmatrix}-1&0&0&0\\0&1&0&0\\0&0&r^2&0\\0&0&0&r^2\sin^2\theta\end{pmatrix}.\tag{A5}$$

To find the orbital plane, we can write

$$\vec{\mathcal{L}}=\mathcal{L}_\perp\hat{\perp}+\mathcal{L}_z\hat{k}=\mathcal{L}_x\hat{i}+\mathcal{L}_y\hat{j}+\mathcal{L}_z\hat{k},\tag{A6}$$

so that we can define

$$\hat{X}\equiv\hat{k}\times\hat{\perp}\qquad\hat{Y}\equiv\hat{\mathcal{L}}\times\hat{X}\qquad\hat{Z}\equiv\hat{\mathcal{L}}.\tag{A7}$$

The orbital plane is spanned by $\hat{X},\hat{Y}$ [19]. Then, the projected coordinates (α,β,γ) of a 3D orbit on the orbital plane are

$$\alpha=\vec{R}\cdot\hat{X},\qquad\beta=\vec{R}\cdot\hat{Y},\qquad\gamma=\vec{R}\cdot\hat{Z}=0.\tag{A8}$$

Therefore, the projection of a 3D orbit onto the orbital plane can be determined by (α,β).

[1] R. Penrose, Phys. Rev. Lett. **14**, 57 (1965).
[2] J. A. Munoz, E. Mediavilla, C. S. Kochanek, E. E. Falco, and A. M. Mosquera, Astrophys. J. **742**, 67 (2011).
[3] B. P. Abbott *et al.* (LIGO Scientific and Virgo Collaborations), Phys. Rev. X **9**, 031040 (2019).
[4] K. Akiyama *et al.* (Event Horizon Telescope Collaboration), Astrophys. J. Lett. **875**, L6 (2019).
[5] K. Akiyama *et al.* (Event Horizon Telescope Collaboration), Astrophys. J. Lett. **930**, L14 (2022).
[6] R. Abuter *et al.* (Gravity Collaboration), Astron. Astrophys. **625**, L10 (2019).
[7] R. Abuter *et al.* (Gravity Collaboration), Astron. Astrophys. **636**, L5 (2020).
[8] T. Clifton, P. G. Ferreira, A. Padilla, and C. Skordis, Phys. Rep. **513**, 1 (2012).
[9] E. Berti, V. Cardoso, and A. O. Starinets, Classical Quantum Gravity **26**, 163001 (2009).
[10] R. A. Konoplya and A. Zhidenko, Rev. Mod. Phys. **83**, 793 (2011).
[11] R. Abbott *et al.* (LIGO Scientific and Virgo Collaborations), Phys. Rev. D **103**, 122002 (2021).
[12] A. Nishizawa, Phys. Rev. D **97**, 104037 (2018).
[13] L. Amarilla, E. F. Eiroa, and G. Giribet, Phys. Rev. D **81**, 124045 (2010).
[14] R. Kumar and S. G. Ghosh, J. Cosmol. Astropart. Phys. 07 (2020) 053.
[15] S.-W. Wei and Y.-X. Liu, Eur. Phys. J. Plus **136**, 436 (2021).
[16] X. Li, X. Zhang, and H.-N. Lin, Phys. Rev. D **106**, 064043 (2022).
[17] K. Glampedakis and D. Kennefick, Phys. Rev. D **66**, 044002 (2002).
[18] J. Levin and G. Perez-Giz, Phys. Rev. D **77**, 103005 (2008).
[19] R. Grossman, J. Levin, and G. Perez-Giz, Phys. Rev. D **85**, 023012 (2012).
[20] V. Misra and J. Levin, Phys. Rev. D **82**, 083001 (2010).
[21] S.-W. Wei, J. Yang, and Y.-X. Liu, Phys. Rev. D **99**, 104016 (2019).
[22] H.-Y. Lin and X.-M. Deng, Eur. Phys. J. C **83**, 311 (2023).
[23] H. Poincaré, Trans. Amer. Math. Soc. **6**, 237 (1905).
[24] L. Lyusternik and A. Fet, Dokl. Akad. Nauk SSSR (N.S.) **81**, 17 (1951).
[25] S. Liu and W. Wang, Acta Math. Sinica, Engl. Ser. **38**, 85 (2022).
[26] D. Bao, S. S. Chern, and Z. Shen, *An Introduction to Riemann-Finsler Geometry* (Springer Press, New York, 2000).
[27] R. Miron and M. Anastasiei, *The Geometry of Lagrange Spaces: Theory and Applications* (Kluwer, Alphen aan den Rijn, Netherlands, 1994).
[28] S. F. Rutz, Gen. Relativ. Gravit. **25**, 1139 (1993).
[29] S. Vacaru, P. Stavrinos, E. Gaburov, and D. Gonta, arXiv:gr-qc/0508023.
[30] C. Pfeifer and M. N. R. Wohlfarth, Phys. Rev. D **85**, 064009 (2012).
[31] E. Kapsabelis, P. G. Kevrekidis, P. C. Stavrinos, and A. Triantafyllopoulos, Eur. Phys. J. C **82**, 1098 (2023).
[32] E. Minguzzi, Phys. Rev. D **95**, 024019 (2017).
[33] C. Lammerzahl, V. Perlick, and W. Hasse, Phys. Rev. D **86**, 104042 (2012).
[34] X. Li and Z. Chang, Phys. Rev. D **90**, 064049 (2014).
[35] X. Li, Phys. Rev. D **98**, 084030 (2018).
[36] X. Li and S.-P. Zhao, Phys. Rev. D **101**, 124012 (2020).
[37] T.-Y. Li, S.-P.Zhao, and X. Li, Phys. Rev. D **105**, 104042 (2022).
[38] A. B. Katok, Izv. Akad. Nauk SSSR Ser. Mat. **37**, 539 (1973) [Math. USSR-Isv. **7**, 535 (1973)].
[39] V. Bangert and Y. Long, Math. Ann. **346**, 335 (2010).
[40] M. Á. Javaloyes and M. Sanch, RACSAM **114**, 30 (2020).
[41] Z. Shen, Manuscr. Math. **109**, 349 (2002).
[42] H.-B. Rademacher, Math. Ann. **328**, 373 (2004).
[43] H. Poincaré, Les méthodes nouvelles de la mécanique céleste: Méthodes de MM. Newcomb, Gyldén, Linstadt et Bohlin (Gauthier-Villars et fils, imprimeurs-libraires, 1893), Vol. **2**.
[44] J. Levin, Classical Quantum Gravity **26**, 235010 (2009).
[45] G. Z. Babar, A. Z. Babar, and Y.-K. Lim, Phys. Rev. D **96**, 084052 (2017).
[46] J. Levin and R. Grossman, Phys. Rev. D **79**, 043016 (2009).
[47] C. W. Misner, K. S. Thorne, and J. A. Wheeler, *Gravitation* (Freeman San Francisco, CA, 2000), pp. 891–901.
[48] W. Schmidt, Classical Quantum Gravity **19**, 2743 (2002).
[49] P. Rana and A. Mangalam, Classical Quantum Gravity **36**, 045009 (2019).